



Use Conditions and Efficiency Measurements of DC Power Optimizers for Photovoltaic Systems

Preprint

Chris Deline
National Renewable Energy Laboratory

Sara MacAlpine
University of Colorado

*Presented at the IEEE Energy Conversion Congress & Expo 2013
Denver, Colorado
September 15–19, 2013*

**NREL is a national laboratory of the U.S. Department of Energy
Office of Energy Efficiency & Renewable Energy
Operated by the Alliance for Sustainable Energy, LLC**

This report is available at no cost from the National Renewable Energy Laboratory (NREL) at www.nrel.gov/publications.

Conference Paper
NREL/CP-5200-59214
October 2013

Contract No. DE-AC36-08GO28308

NOTICE

The submitted manuscript has been offered by an employee of the Alliance for Sustainable Energy, LLC (Alliance), a contractor of the US Government under Contract No. DE-AC36-08GO28308. Accordingly, the US Government and Alliance retain a nonexclusive royalty-free license to publish or reproduce the published form of this contribution, or allow others to do so, for US Government purposes.

This report was prepared as an account of work sponsored by an agency of the United States government. Neither the United States government nor any agency thereof, nor any of their employees, makes any warranty, express or implied, or assumes any legal liability or responsibility for the accuracy, completeness, or usefulness of any information, apparatus, product, or process disclosed, or represents that its use would not infringe privately owned rights. Reference herein to any specific commercial product, process, or service by trade name, trademark, manufacturer, or otherwise does not necessarily constitute or imply its endorsement, recommendation, or favoring by the United States government or any agency thereof. The views and opinions of authors expressed herein do not necessarily state or reflect those of the United States government or any agency thereof.

This report is available at no cost from the National Renewable Energy Laboratory (NREL) at www.nrel.gov/publications.

Available electronically at <http://www.osti.gov/bridge>

Available for a processing fee to U.S. Department of Energy and its contractors, in paper, from:

U.S. Department of Energy
Office of Scientific and Technical Information
P.O. Box 62
Oak Ridge, TN 37831-0062
phone: 865.576.8401
fax: 865.576.5728
email: <mailto:reports@adonis.osti.gov>

Available for sale to the public, in paper, from:

U.S. Department of Commerce
National Technical Information Service
5285 Port Royal Road
Springfield, VA 22161
phone: 800.553.6847
fax: 703.605.6900
email: orders@ntis.fedworld.gov
online ordering: <http://www.ntis.gov/help/ordermethods.aspx>

Cover Photos: (left to right) photo by Pat Corkery, NREL 16416, photo from SunEdison, NREL 17423, photo by Pat Corkery, NREL 16560, photo by Dennis Schroeder, NREL 17613, photo by Dean Armstrong, NREL 17436, photo by Pat Corkery, NREL 17721.



Printed on paper containing at least 50% wastepaper, including 10% post consumer waste.

Use Conditions and Efficiency Measurements of DC Power Optimizers for Photovoltaic Systems

Chris Deline

National Renewable Energy Laboratory
Golden, Colorado, USA
chris.deline@nrel.gov

Sara MacAlpine

University of Colorado
Boulder, Colorado, USA
sara.macalpine@colorado.edu

Abstract—No consensus standard exists for estimating annual conversion efficiency of DC-DC converters or power optimizers in photovoltaic (PV) applications. The performance benefits of PV power electronics including per-panel DC-DC converters depend in large part on the operating conditions of the PV system, along with the performance characteristics of the power optimizer itself. This work presents a case study of three system configurations that take advantage of the capabilities of DC power optimizers. Measured conversion efficiencies of DC-DC converters are applied to these scenarios to determine the annual weighted operating efficiency. A simplified general method of reporting weighted efficiency is given, based on the California Energy Commission’s CEC efficiency rating and several input / output voltage ratios. Efficiency measurements of commercial power optimizer products are presented using the new performance metric, along with a description of the limitations of the approach.

I. INTRODUCTION

The fast-growing field of photovoltaic (PV) power generation has seen great innovation in its balance-of-system (BOS), including the introduction of power electronics devices which are applied at the panel level. The devolution of power conversion from central inverters to the panel level has been shown to improve performance due to reduced PV module mismatch [1-3]. Prior estimates of performance improvement from the use of distributed power electronics indicate that the potential for mismatch power recovery depends greatly on the site-specific details of the PV installation [4-6]. Additional potential benefits of distributed power electronics include increased design flexibility by allowing mismatched or longer strings of PV panels, improved monitoring, and increased system availability [7-9]. Despite these potential benefits, a critical factor in distributed power converters’ utility is their conversion efficiency, which needs to be high in order to compete with conventional centralized inverter approaches [10].

For distributed AC products such as microinverters, a weighted DC-to-AC conversion efficiency can be measured by the CEC [11] or EN50530 (European) [12] inverter efficiency method. However, no consensus standard exists for estimating the annual weighted efficiency of DC-DC converter devices, also known as power optimizers. Existing

inverter measurement methods use a weighted average of the inverter performance over a range of input power P_{in} / P_{max} and input voltage V_{in} / V_{max} where subscript $_{max}$ denotes maximum rated power or voltage. However, power optimizers have an additional free parameter, the voltage ratio $M = V_{out} / V_{in}$. This additional variable is unaddressed by any present power rating standard. A proposal is given in [13] to apply existing inverter standards to power optimizers by averaging conversion efficiency η over the entire range of M , and applying the appropriate power rating. However, this approach will likely underestimate η for power optimizers, which may operate near $V_{out} / V_{in} = 1$ under many use conditions, as will be shown here.

This work examines the conversion efficiency of DC power optimizers, and usage scenarios that will help to define common metrics for defining and comparing weighted conversion efficiency. The paper is arranged as follows: in Section II, measured efficiency curves of commercial power optimizer devices are provided to investigate the dependence of η on voltage and power operating conditions. In Section III, typical use scenarios are described for power optimizer devices. In Section IV, a computer simulation is described, which is used to create annual operating histograms to determine the amount of power processed by power optimizers under different use conditions. Section V discusses different methods of providing weighted efficiency, with comparison to the scenarios investigated here.

II. POWER OPTIMIZER EFFICIENCY MEASUREMENT

To illustrate how η is a function of both input power and V_{out} / V_{in} , efficiency plots for a commercial DC-DC converter (National Semiconductor SM1230-3A1) are shown in Figure 1. Conversion efficiency for this device is determined by measuring input and output voltage and current to 0.1% accuracy using a Keithley 2701 DMM, with input voltage provided by a solar array simulator (Agilent E4363-J02), and output power dissipated in a digital electronic load (NHR 4760-1kW). Each input power and output voltage condition is monitored over a period of 5 minutes to determine the average η for each operating point. The effect of higher or

This work was supported by the U.S. Department of Energy under Contract No. DOE-AC36-08GO28308 with the National Renewable Energy Laboratory.

This report is available at no cost from the National Renewable Energy Laboratory (NREL) at www.nrel.gov/publications.

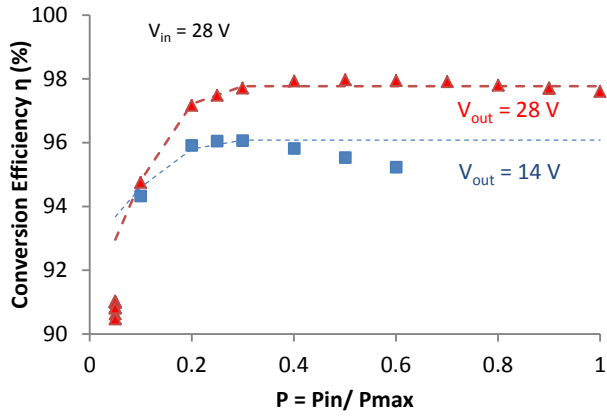
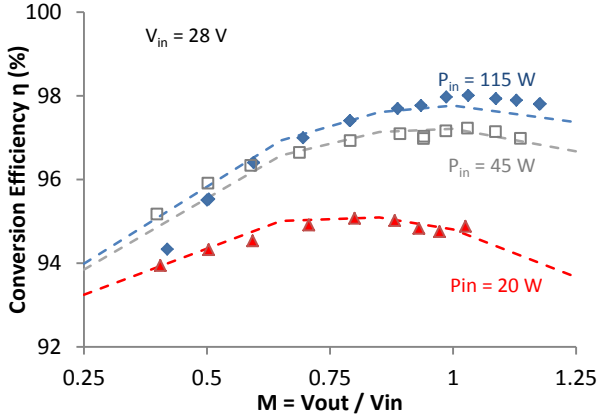


Figure 1. Measured conversion efficiency η of a commercial DC power optimizer at three input power levels (top) and at two output voltages (bottom). Maximum rated power: 230W. Modeled efficiency is shown as a dashed line.

lower values of V_{in} was investigated for constant V_{out} / V_{in} , but this was not found to have a strong impact on η .

An empirical model is developed for the various power and voltage operating conditions of this power converter, with modeled results shown as dashed lines in Figure 1. This empirical model is employed to assist in device performance simulations in Section IV of this work. The empirical equation approximating this device's conversion efficiency is:

$$\eta = 0.977 (0.932 + C_2 M - 0.068 M^2) \quad (1)$$

Where C_2 is a constant based on $P = P_{in} / P_{max}$:

$$C_2 = 0.064 + 0.51 P - 0.88 P^2 \text{ for } P < 0.25 \quad (2)$$

$$C_2 = 0.1365 \text{ for } P \geq 0.25$$

Two additional commercial DC converter devices were measured to compare with the results of Figure 1, labeled here as Conv2 and Conv3. These additional measurements

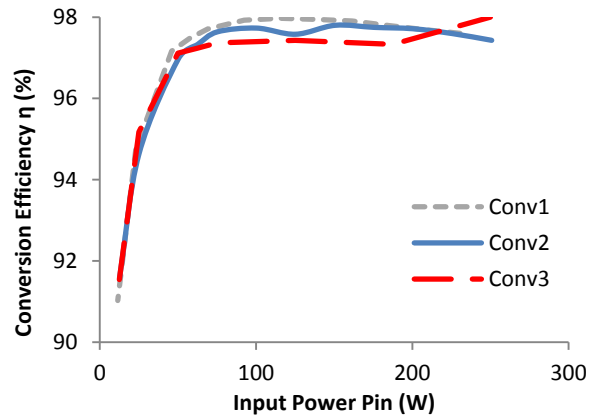
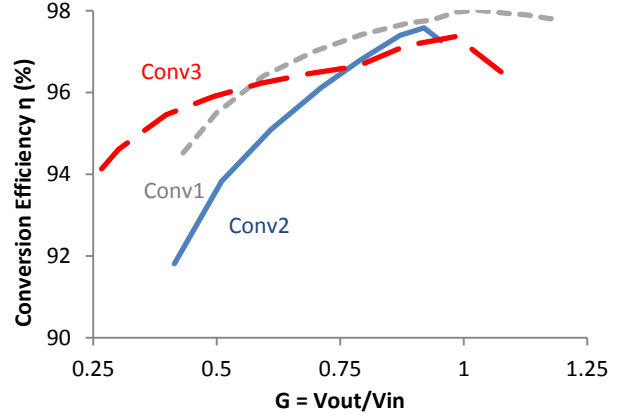


Figure 2: Measured conversion efficiency of three commercial DC power optimizers at 50% rated input power (top) and at output voltage $V_{out} = V_{in}$ (bottom). Conv1 is the same converter shown in Figure 1 (National Semiconductor SM1230-3A1).

in Figure 2 show a similar decrease in efficiency with low input power and output voltage, even though Conv2 is a buck-only converter, and Conv1 and Conv3 are buck-boost converters.

III. TYPICAL USE SCENARIOS OF DC POWER OPTIMIZERS

The potential use cases of DC power optimizers are limitless, however we will focus on two main applications: partial shading mismatch mitigation, and string length optimization. While the first application has received the most attention to date, the second is increasingly of interest for large-scale unshaded PV systems due to potential reduction of BOS costs. All scenarios here assume a fixed-tilt PV installation.

A. Scenario 1: Partial shading mismatch reduction

The performance benefit of distributed power electronics in partially shaded PV systems is well documented [1-10]. Partial shading in PV systems leads to losses due to reduced irradiance, and due to mismatch in operating point between panels. It is this second power loss that is recovered through the use of distributed power electronics, and can make up

15% - 50% of the total annual shading power loss, depending on the extent of shade and system configuration [4].

To determine a representative amount of shade to consider here, site survey information was obtained from a large residential installer in California, showing the extent of shade on 66 residential PV installations [14]. In these installations, a panoramic view of surrounding obstructions was taken, and the annual irradiance lost due to shade was calculated. Here, annual irradiance is defined as “Solar Access” measured by a Solmetric Suneye imaging tool [15]. This measurement was averaged across each installation using multiple images taken at the corners of the PV array. The annual shading losses for these various site surveys are given in Figure 3.

For the typical use scenario considered here, we are focusing on a ‘moderate’ shading case, highlighted in Figure 3, and described in more detail in [3]. The 19% annual shade loss in this case is greater than average, and perhaps typical of sites that would benefit from distributed power electronics. Shade is cast by several nearby trees, primarily in the early morning and late afternoon. In this scenario, we assume a residential roof-mount PV system, 2.9 kW in size composed of 14 Sharp ND-208 modules in two parallel strings. The system is assumed to be equipped with DC power optimizers based on the measured performance of Conv1, namely a buck-boost converter with conversion efficiency following Eq. (1) and Eq. (2). The PV strings are assumed to be connected to a conventional string inverter with a wide DC voltage input window from 150 – 500 V. Note that while a buck-boost power optimizer is assumed in this simulation, a buck-only converter could be substituted with little change in the analysis, although the shade mitigation capabilities would be diminished somewhat [4].

B. Scenario 2 & 3: 30% and 100% String Expansion

The use of DC power optimizers can enable improved performance and reduced cost in another way – by increasing the number of PV modules in a series string, thus reducing

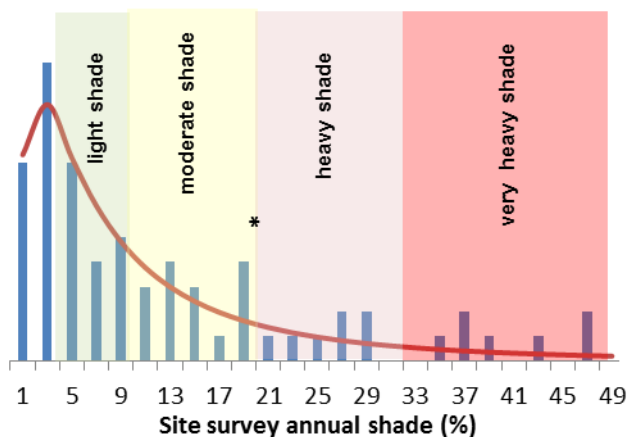


Figure 3. Site survey details for 66 residential installations. Distribution best fit is log-normal with $\mu = 2.025$ and $\sigma = 1.11$. The asterisk * indicates the amount of shade for the shaded installation discussed here.

the total number of strings for a given PV system size. This reduces per-string costs associated with homerun wiring, fuses, and DC combiner boxes, and reduces resistive power loss because of higher DC bus voltage. DC-DC converters provide this capability because the length of a PV string is conventionally limited by the maximum system V_{oc} on the coldest day [16]. However, by integrating converters with buck capability, the system operating voltage can be maintained below this threshold, even if there are a larger number of PV modules in the series string [17].

Two case studies of string lengthening are considered here: a 30% elongation case (Scenario 2), and a 100% elongation case (Scenario 3). In both cases, the increased string length is based on a default conventional PV string sized for a 1000V commercial installation, again using Sharp ND-208 PV modules as in section 3.1. Because of the module’s V_{oc} and V_{mp} parameters of 36 V and 28.5 V respectively, a conventional series string would have a maximum of 23 modules, to remain below 1000V at a low temperature of -25 °C. With the use of DC-DC converters however, a 30% longer string of 30 PV modules is possible for Scenario 2, and a 100% longer string of 46 modules is chosen for Scenario 3. To limit complexity, mismatch between strings is assumed to be negligible in this case study. As with Scenario 1, each PV module in the system is equipped with converter Conv1.

A critical aspect of the string lengthening study is the capability of the DC-AC inverter connected to the PV strings. The inverter’s DC voltage range will dictate operating conditions experienced by the module-level electronics. For this 1000V commercial system, a central inverter with wide maximum power tracking (MPPT) range is assumed – 500V – 850V. However, in the 100% elongation case, the PV string voltage is so far above the inverter DC input spec that the inverter can be considered to have a fixed DC input voltage of 850V. The use of high fixed-input-voltage inverters can result in additional performance and cost improvements [18].

IV. SIMULATION OF POWER OPTIMIZER OPERATING CONDITIONS

A. Partial shading simulation method

A detailed analysis is conducted of the moderate shading case described in [14] to estimate the operating conditions of either buck or buck-boost power optimizers under such shading conditions. The irradiance-weighted histogram of operating conditions for the different power optimizers in the system forms the basis for a weighted efficiency measurement.

A ray-tracing analysis is conducted to estimate the cell-level and module-level irradiance on the system, based on irradiance data for a nearby site in Denver, CO. Partial shading is assumed to block the direct-beam component of irradiance, allowing diffuse irradiance to still reach the shaded portion of the module. The performance of the buck-boost power optimizer Conv1 is modeled based on its ideal

behavior as described in [19]. Output power $P_{out} = \eta P_{in}$ where η is conversion efficiency, determined from Eq. (1) and (2) above. Additional assumed operating constraints of Conv1 include a fixed maximum output voltage of $V_{out} = 50$ V and $I_{out} = 9$ A.

Input conditions to the power optimizer are determined by scaling the module's V_{mp} and I_{mp} based on the Sandia array performance coefficients [20]. The Sandia model takes meteorological inputs including temperature, wind speed and the reduced irradiance E_e , based on the plane-of-array irradiance G_{POA} and the 1000 W/m² reference irradiance G_{ref} . Shading is accounted for by determining the fraction of a module covered by shade. For each 1/3 of a module containing shade (representing the 3 bypass-diode protected submodules), the input power is reduced by 1/3. If more than 1/3 of a module contains shade, the module is assumed to operate at a low-current, high-voltage local maximum point, such that $E_e = G_d / G_{ref}$ where G_d is the diffuse irradiance. This accounts for real-world input voltage limits of available power optimizer devices. Note that temperature is assumed to be constant across the array.

B. String lengthening simulation method

Annual performance conditions of the modules in Scenarios 2 and 3 are based on measured PV performance of a crystalline silicon module deployed at NREL's Outdoor Test Facility. These data are measured every 15 minutes over a year's deployment, with power-weighted distributions of module temperature, V_{mp} and P_{mp} shown in Figure 4. Note that for consistency the measured PV current and voltage parameters are scaled to match the nameplate ratings of the 208W Sharp panel used in this work.

To generate annual operating histograms of DC power optimizers in the two string lengthening scenarios, the

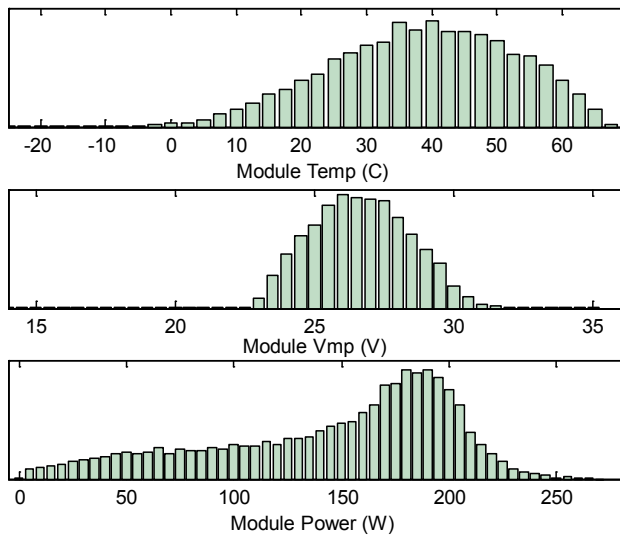


Figure 4. Module temperature (top) V_{mp} distribution (center) and P_{mp} distribution (bottom) of one year's deployment of an open-rack crystalline - Si PV module. Parameters are scaled to match nameplate parameters of a Sharp ND-208 module, and weighted by power.

converters' V_{in} is determined directly by scaled experimental V_{mp} of the modules. Each converter's module level V_{out} is assumed equal to V_{in} so long as the associated string voltage lies within the inverter MPPT range of 500-850 V; otherwise string voltage is clamped to the upper or lower limit (typically the upper limit in these scenarios), and the module level V_{out} is scaled proportionally. P_{in} for each converter is also determined directly by the module's scaled experimental P_{mp} . Efficiency η is calculated based on Eq. (1) and (2). In generating operating histograms of $M = V_{out} / V_{in}$ and weighted efficiency, values at each time point are weighted by P_{in} to reflect their contribution to cumulative energy in kWh.

V. SIMULATION RESULTS

Results of annual simulations are distilled into histograms of the operating conditions seen by the power optimizers in each of the three scenarios. Two operating conditions in particular are required for calculation of weighted efficiency according to Eq. (1) and (2): input power and $M = V_{out} / V_{in}$. The next two sub-sections will discuss these annual operating conditions for the three scenarios, along with annual conversion efficiency based on these histograms.

A. Simulation results: Power histogram

An annual histogram of the module-level power optimizers' input power P_{in} is given in Figure 5 for the three scenarios. Also plotted in Figure 5 is the CEC efficiency scaling for inverter static efficiency, given by:

$$P_{CEC} = 0.04 P_{10\%} + 0.05 P_{20\%} + 0.12 P_{30\%} + 0.21 P_{50\%} + 0.53 P_{75\%} + 0.05 P_{100\%} \quad (3)$$

where $P_{XX\%}$ indicates input power in Watts at $XX\%$ of the maximum power optimizer output, set here to $P_{100\%} = 245$ W. Both CEC plot and scenario histograms are scaled to a total annual probability of 1.

Figure 5 shows that there is a slight difference between the modeled power histograms and the CEC weighting,

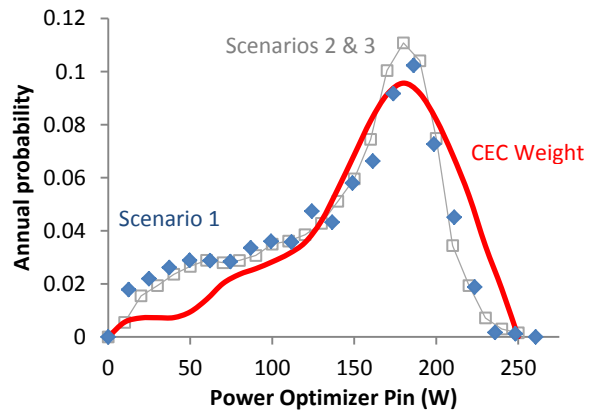


Figure 5. Power-weighted P_{in} histogram of the module-level power optimizers for a full year simulation, Scenarios 1 - 3. The power weighting for the CEC inverter test method is shown for reference.

however the general shape remains the same. For the shaded histogram of Scenario 1, there is a flattening of the distribution and a shift towards lower P_{in} . This reduction in P_{in} can be understood as the effect of partial shading on the system, dropping the production of shaded modules for a portion of the time while the system experiences partial shading. The unshaded histogram of Scenario 2 & 3 indicates that there may also be climactic differences between these simulations (Denver, CO) and the California location chosen for the CEC weighting.

B. Simulation results: V_{out} / V_{in} and η histogram

The second operating histogram required to calculate power optimizer η is $M = V_{out} / V_{in}$ which is shown in Figure 6 for the three scenarios. Again, histogram counts are scaled by P_{out} and normalized such that total annual probability = 1. For Scenarios 1 & 2, operation at $M = 1$ is much more prevalent than any other operating mode. $M = 1$ accounts for 60% of the annual kWh produced for the Scenario 1 simulation, and 83% of annual kWh for the Scenario 2 simulation. For Scenario 3, the distribution was not centered at $V_{out} / V_{in} = 1$, instead having a more broad distribution between $M = 0.7 - 0.8$. This is due to the inherent mismatch between the string V_{mp} of 1300 V and the inverter's input voltage of 850 V, requiring the power optimizers to constantly operate in buck mode to match the string voltage to the inverter input voltage.

Given the annual operating conditions of Figure 5 and Figure 6, DC converter efficiency η can be calculated for each scenario with Eqs. (1) and (2). An annual histogram of η is compiled for each use scenario, and shown in Figure 7. The partially shaded installation of Scenario 1 and the 30% elongated string system of Scenario 2 each have similar efficiency distributions, centered around $\eta = 0.978$. The efficiency distribution of Scenario 3 is shifted to lower efficiency, due to the large percentage of time operating at $M \neq 1$.

The η histograms of Figure 7 can be integrated to obtain annual power-weighted efficiency of the DC-DC converter

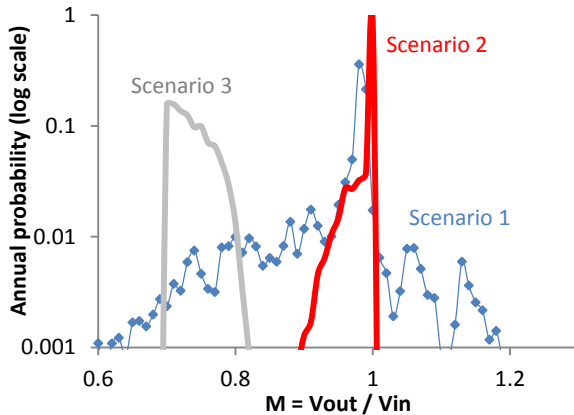


Figure 6. Annual histogram of V_{out} / V_{in} , three power optimizer scenarios. Histogram is scaled by P_{in} and plotted on a log scale. Scenarios 1 and 2 are peaked and centered at $M = 1$. Scenario 3 has a maximum at $M = 0.7$.

in each of the three scenarios considered. These integrated values are shown below in Table I.

TABLE I. ANNUAL SIMULATED EFFICIENCY OF DC POWER OPTIMIZER CONV1 IN THREE SCENARIOS

Scenario #	Power-weighted η
1: Partial shading	97.5 %
2: 30% Longer String	97.6 %
3: 100% Longer String	97.0 %

VI. ALTERNATE WEIGHTED EFFICIENCY CALCULATION

Section V illustrated a method for calculating weighted efficiency of a DC power optimizer for specific scenarios. However, detailed knowledge of an intended use scenario is not necessarily available. Also, to be generally usable, calculations of power optimizer efficiency (which could be included in datasheets, etc) should represent a wide range of operating conditions, yet require only limited data measurement points.

For these reasons, a proposed standard weighted efficiency method is suggested which does not require site-specific power or V_{out} / V_{in} histograms. Instead, more general functions for both P_{in} and M are used. Several measurement options will be considered, with the impact on calculated η compared with full simulated η 's of Table I.

A. General P_{in} histogram

Close agreement between Eq. (3) and simulated power histograms (Figure 5) suggests that we use the existing CEC power weighting method for our standardized η measurement. Eq. (3) provides the values of P_{in} at which η measurements are made, and the weight to apply to each measurement. This power weighting is most accurate for similar fixed-tilt, high irradiance locations.

B. General $M = V_{out} / V_{in}$ histogram

An impediment to determining a general histogram for M is that the use scenario greatly affects the shape of M . We

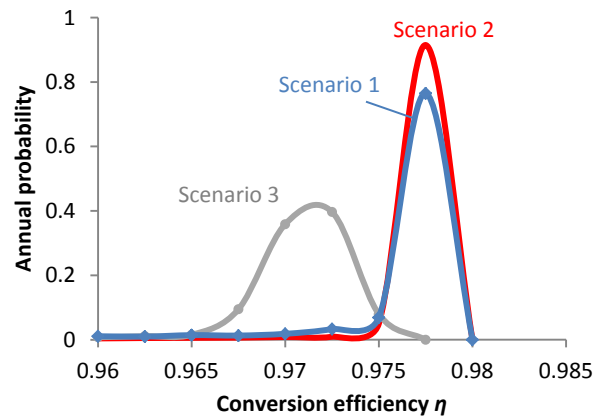


Figure 7. Annual power-weighted conversion efficiency for the three power optimizer scenarios.

will begin by assigning a general histogram to apply in cases such as for Scenario 1 and Scenario 2, then discuss possible histogram choices for cases such as Scenario 3.

As shown by the peaked V_{out} / V_{in} distributions for Scenario 1 and Scenario 2 (Figure 6), DC power optimizers operate under $M = 1$ conditions for a majority of the time, even in PV systems with moderate partial shading. This will generally be true for PV systems where the string V_{mp} is within the inverter’s input voltage window; for instance, where PV strings are designed to have equal length, and where string length is chosen by conventional methods, or with a moderate increase in string length $\leq 30\%$. For these cases, M can be modeled relatively closely by a single-point distribution at $M = 1$, since probability drops off rapidly for $M \neq 1$. Therefore, the first standard η measurement method considered here is one where each power measurement condition of Eq. (3) is taken at the single point $M = 1$.

However, as is shown by the analysis of Scenario 3, when a significant mismatch exists between the string voltage and the inverter input voltage, DC power optimizers play a more active role in mitigating mismatch. This would also be the case if PV strings of unequal length are connected to the same inverter channel. In these constant mismatch cases, power optimizers operate continuously at $M \neq 1$.

For systems resembling Scenario 3, where string V_{mp} is outside the inverter’s MPPT range, a different annual histogram for M may be more appropriate. Of course, a site-specific distribution would be ideal, but in this study we consider two general distributions: a uniform distribution assigning equal weight for all values of M across the conversion range of the device from $M = 0.25$ to $M = 1.25$ (suggested in [13]), and a linear triangle distribution, peaked at $M = 1$ and reaching a probability of zero at $M = 0.25$ (suggested in [21]). These general distributions are illustrated in Figure 8 along with the single-point voltage distribution already discussed.

By measuring the efficiency of Conv 1 at each combination of CEC power value (Eq. 3) and value of M called out in Figure 8, one may calculate a non-site-specific

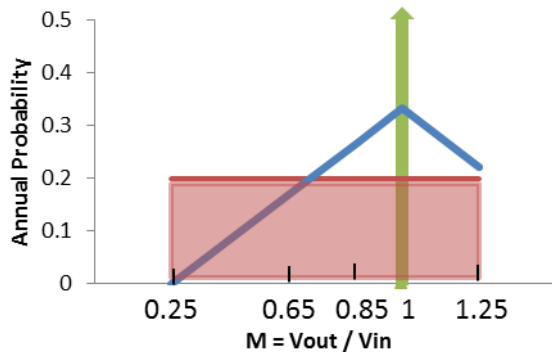


Figure 8. General M distributions considered for a weighted efficiency method. Green line is single-point $M = 1$ distribution for Scenarios 1 & 2. Red box is a uniform distribution. Blue lines indicate a triangle distribution.

TABLE II. EXPERIMENTAL η OF CONV1 POWER OPTIMIZER, EVALUATED WITH FOUR WEIGHTING METHODS.

	CEC, $M = 1$	CEC, Uniform M	CEC, Triangle M	Max efficiency
Scenario 1: 97.5 %	97.6%	96.7%	97.3 %	98.0%
Scenario 2: 97.6 %	97.6%	96.7%	97.3 %	98.0%
Scenario 3: 97.0 %	97.6%	96.7%	97.3 %	98.0%

weighted converter efficiency. The measured weighted efficiency values resulting from these three distributions are given in Table II.

C. Comparison of weighted efficiency methods

Table II shows a comparison between the site-specific simulated η values of Table I and the proposed weighted efficiency distributions as described above. Weighting values are applied at the P_{in} / P_{max} values shown in Eq. (3) and the V_{out}/V_{in} values of $M = [0.25, 0.65, 0.85, 1, 1.25]$. Three distributions of M are represented along with a single-point η value based on the maximum efficiency measured during the test.

The most accurate general method for calculating η for each scenario is highlighted in green. For Scenarios 1 and 2, the $M = 1$ distribution provides an estimate of η that matches particularly well. The fact that these two scenarios (partial shading and 30% string lengthening) operate for a great deal of time at $M = 1$ means that neglecting other M operating conditions has limited impact on η calculation accuracy. However, Scenario 3 has an annual weighted efficiency that is much lower than the other two scenarios, and is not modeled particularly well by either the Uniform or Triangle distribution of Figure 8. Scenario 3 would best be represented by a uniform distribution from $M = 0.7 - 0.8$, or a single-point value of M in that range. It would be more appropriate to utilize a site-specific distribution for M in the case of such a large mismatch between string V_{mp} and the inverter input window.

In all scenarios the maximum measured efficiency of 98.0% is not representative of the weighted efficiency, since it does not represent the total operating conditions experienced by power optimizers in real PV installations.

VII. CONCLUSIONS

Weighted power optimizer conversion efficiencies have been presented based on three scenarios, including a moderately shaded scenario and two ‘string lengthening’ scenarios. The power optimizer conversion efficiency was found to depend greatly on how well matched the inverter input voltage was with the PV string V_{mp} . For PV systems with a designed string-level V_{mp} within the inverter’s input voltage window, a site-independent measurement method was described for simplified weighted efficiency calculation. Namely, the CEC power weighting should be used, along with a single-point $M = 1$ voltage distribution. However, for

systems using fixed input voltage inverters, or those with significant voltage mismatch between parallel strings, a site-dependent analysis may be required for accurate conversion efficiency estimates, since significant site-to-site variation may exist in the annual weighted efficiency.

REFERENCES

- [1] C. Podewils and M. Levitin, "Hidden powers," Photon magazine, November 2010
- [2] M. Gross, S. Martin and N. Pearsall, "Estimation of Output Enhancement of a Partially Shaded BIPV Array by the use of AC Modules," in 26th IEEE Photovoltaic Specialists Conference, 1997
- [3] C. Deline, "Partially Shaded Operation of Multi-String Photovoltaic Systems," IEEE Photovoltaic Specialists Conference, Honolulu, HI, 2010.
- [4] C. Deline, B. Marion, J. Granata and S. Gonzalez, A Performance and Economic Analysis of Distributed Power Electronics in Photovoltaic Systems. NREL Report No. TP-5200-50003. Golden, CO: National Renewable Energy Laboratory, December 2010. <http://www.nrel.gov/docs/fy11osti/50003.pdf>.
- [5] S. MacAlpine, R. Erickson and M. Brandemuehl, "Characterization of Power Optimizer Potential to Increase Energy Capture in Photovoltaic Systems Operating Under Nonuniform Conditions," IEEE Transactions on Power Electronics **28** pp 2936-2945, 2013
- [6] S. Poshtkouhi, V. Palaniappan, M. Fard, and O. Trescases, "A general approach for quantifying the benefit of distributed power electronics for fine grained mppt in photovoltaic applications using 3-d modeling," IEEE Transactions on Power Electronics, vol. 27, no. 11, pp. 4656–4666, 2012.
- [7] N. Femia, G. Lisi, G. Petrone, G. Spagnuolo and M. Vitelli, "Distributed Maximum Power Point Tracking of Photovoltaic Arrays: Novel Approach and System Analysis," in IEEE Transactions on Industrial Electronics, Vol. 55, No. 7, July 2008, pp. 2610-2621.
- [8] B. Burger, B. Goeldi, S. Rogalla and H. Schmidt, "Module Integrated Electronics – An Overview," in 25th European Photovoltaic Solar Energy Conference and Exhibition, 2010.
- [9] A. Elasser, M. Agamy, J. Sabate, R. Steigerwald, R. Fisher and M. Harfman-Todorovic "A Comparative Study of Central and Distributed MPPT Architectures for Megawatt Utility and Large Scale Commercial Photovoltaic Plants," Proceedings of Industrial Electronics Conference(IECON) 2010, pp. 2753-2758.
- [10] M. Agamy, M. Harfman-Todorovic, A. Elasser, J. Sbate, R. Steigerwald, Y. Jiang and S. Essakiappan, "DC-DC Converter Topology Assessment for Large Scale Distributed Photovoltaic Plant Architectures," proceedings, IEEE Energy Conversion Congress and Exposition, 2011
- [11] W. Bower, C. Whitaker, W. Erdman, M. Behnke, and M. Fitzgerald. Performance test protocol for evaluating inverters used in grid-connected photovoltaic systems, 2004, available online at http://www.energy.ca.gov/renewables/02-REN-1038/documents/2004-12-01_INVERTER_TEST.PDF
- [12] EN 50530, Overall efficiency of PV inverters, CENELEC, December 2008
- [13] R. Bründlinger, N. Henze, G. Lauss and J. Liu, "Module integrated power converters – a comparison of state-of-the-art concepts and performance test results," 26th European Photovoltaic Solar Energy Conference and Exhibition, 2011
- [14] Solar Works. Private communication. August 2011.
- [15] Solmetric Inc. "Application Note: Understanding the Solmetric SunEye," March 2011. <http://resources.solmetric.com/get/UnderstandingTheSolmetricSunEye-March2011.pdf>.
- [16] 2008 National Electrical Code, Section 690.7 National Fire Protection Association, Inc., Quincy, MA, 2002.
- [17] L. Gun, "Module Level Power Management Decreases PV Costs and Risks," Proceedings, ASES World Renewable Energy Forum, 2012
- [18] HDPV alliance website, <http://www.hdpv.org/>
- [19] P. Tsao, "Simulation of PV systems with power optimizers and distributed power electronics," 35th IEEE Photovoltaic Specialists Conference (PVSC), 2010.
- [20] D.L. King, W.E. Boyson, J.A. Kratochvil, "Photovoltaic array performance model," Sandia Report No. SAND2004-3535, 2004
- [21] SolarEdge. Private communication. May 2013.